Technical Note

One-Sided Impact Spatter and Area-of-Origin Calculations

Andy Maloney [1]
Céline Nicloux [2]
Kevin Maloney [3]
Franck Heron [2]

Abstract: It is common practice when calculating area of origin from impact spatter to use stains from both "sides" of the pattern – stains to the left and to the right of the blood source. Impact spatter at crime scenes, however, often provides the analyst with bloodstain patterns that are not as pristine as those created in a controlled environment. One situation that may arise is impact spatter consisting of stains from only one side of the pattern because of the removal of an object after the impact, such as a door or a person, or because the stains from one side are not on a planar surface. This study looks at a method of calculating the area of origin using stains from only one side of the pattern and shows that these partial patterns may still provide usable calculations to determine the area of origin.

Introduction

Bloodstain pattern analysts often have to deal with less than ideal situations when attending a crime scene. Sometimes they are presented with incomplete information, which may mean they exclude it completely from their crime scene analysis. In certain situations, however, even this incomplete information may assist the analyst.

[1] FORident Software, Inc.
[2] L'Institut de Recherche Criminelle de la Gendarmerie Nationale, France
[3] Forensic Identification Section, Ottawa Police Service, Ottawa, ON, Canada

Received May 12, 2010; accepted August 23, 2010

One such situation arises when the analyst is presented with only one part of an impact pattern. Typically, when analyzing an impact pattern, stains are chosen from all primary zones surrounding the general area of the blood source [1], resulting in some stains with positive gamma angles (right of center) and some with negative gamma angles (left of center). Sometimes, however, analysts are only able to find usable stains from one side of a pattern, resulting in stains with all positive or all negative gammas. This may be the result of an object being moved after the impact, stains that are not on planar surfaces, or simply because no suitable stains may be found.

Calculating the area of origin of an impact pattern consists of projecting the three-dimensional vectors representing the trajectories onto the x-y plane, determining their intersection points, calculating the average x and y, and then using the plane calculated from this point to calculate the average height (z). In a typical two-sided impact pattern analysis, the method of determining the intersection points is to iterate over the negative gamma trajectories looking for intersections against each of the positive gamma trajectories [2, 3]. This means that intersections between any two negative gamma trajectories or any two positive gamma trajectories are not used in the calculation.

For this study, we split each full two-sided pattern into two groups – those trajectories with positive gammas, and those with negative gammas. Each of these groups was then considered a separate pattern for the purposes of analysis. For the area-of-origin calculations, we explicitly allowed intersections between same-side trajectories. Thus, to calculate the area of origin for these new one-sided patterns, we iterated over all the trajectories in the new pattern looking for intersections against each other.

This study was undertaken to explore what information may be extracted from these "one-sided" impact patterns and to determine whether it could provide usable information to the analyst.

Materials and Methods

For this study, a controlled environment was constructed at L'Institut de Recherche Criminelle de la Gendarmerie Nationale (IRCGN) in Paris, France. The target area consisted of three walls of white melamine board (Figure 1), though all impacts were generated on the front wall. For each impact, a new sheet

of kraft paper measuring 1.0 m x 1.5 m was taped to the wall at a known location (y = 25.0 cm, z = 65.0 cm). A rectangular area was marked on the wall at that location to allow us to place a sheet of paper in the same spot for each impact. The left edge of this rectangular area was perpendicular to the bottom edge of the wall, and the bottom edge of the rectangular area was parallel to the bottom edge of the wall (Figure 2).

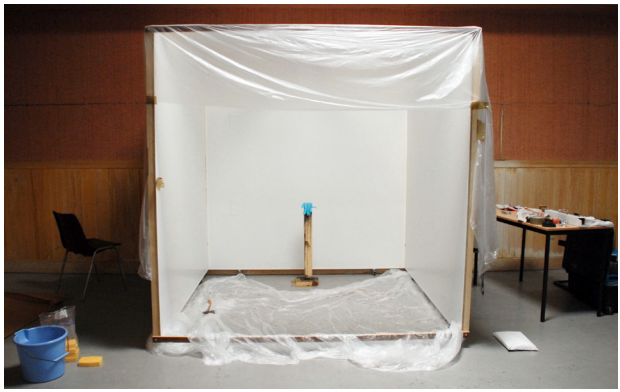

Figure 1

A target area was constructed for this experiment.

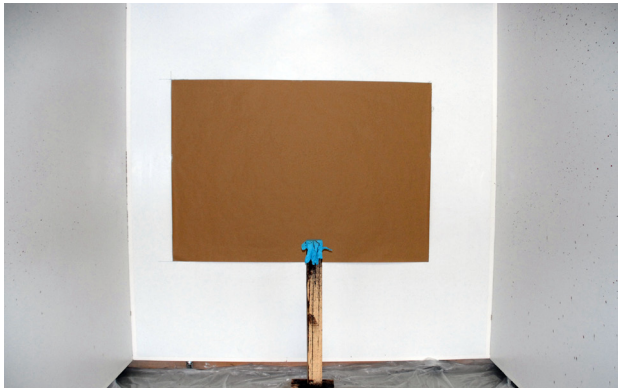

Figure 2

Targets were taped to the wall in a marked-off location.

A wooden post with an official Team Canada hockey puck nailed to the top was used as a striking surface (Figure 3). This was placed at a known location marked on the floor with tape, and the puck was wiped clean after each strike. For each of the strikes, the center of the puck was located at x = 30.0 cm, y = 103.8 cm, and z = 83.0 cm.

We used human blood containing a CPD (citrate phosphate dextrose)/SAGM (saline adenine glucose mannitol) anticoagulant solution. This was acquired from the Centre de Transfusion Sanguine des Armées (CTSA) from their expired blood transfusion stock. A pipet was used to place 1.5 mL of blood on the puck in the same location for each impact. One analyst performed each of the strikes using a wooden-handled hammer (Figure 3).

In all, 32 impact patterns – labeled "Pattern A" through "Pattern AF" – were created in this controlled environment, giving 64 "one-sided" patterns to analyze for the study. Instead of generating and then analyzing one pattern at a time, we chose to generate and collect the data in a batch process. This meant generating all the patterns first, then doing stain selection and adding plumb lines to each of them, then doing all the photography, and finally measuring the location of each stain. This workflow allowed us to complete the creation and data collection for all 32 impact patterns in a relatively short time.

After all 32 patterns were created and allowed to dry, a minimum of 20 stains were selected from each pattern for analysis – giving us at least 10 stains per side – and scales were placed on the sheet of paper for each stain. The stains were selected on the basis of their size, shape, and location. The same analyst performed stain selection on all patterns.

Right angle rulers were used to position and draw plumb lines for each of the stains. The bottom edge of the ruler was lined up against the edges of the sheet of paper, and plumb lines were drawn on the stain's scale with a marker. Two analysts worked on adding plumb lines while the other analyst was performing stain selection.

To photograph the stains, each pattern's sheet of paper was placed flat on a large table. A clear plexiglass tube 28 cm in length was attached to a Nikon D200 camera with a 18–35 mm lens to photograph the stains (Figure 4). When placed straight down over the stain, this tube ensured that the focal plane of the camera was parallel to the sheet of paper. This eliminated any pitch or yaw of the camera's lens with respect to the stain on the surface which distorts the stain image and may affect the

analysis of the stain. As with a normal analysis, a plumb line was used to correct for camera roll. Two crime lights were used to enhance the lighting because we found that the flash could not be used effectively with the plexiglass tube (Figure 4). One analyst took the photos while the other two manipulated the lights.

Figure 3

A hockey puck was used as a striking surface and a wooden-handled hammer as the striking instrument.

Figure 4

A plexiglass tube was attached to the camera and the stains were lit with two crime lights.

To measure the stain locations, a right angle border was constructed out of plastic and secured to the table. Aligning the sheets of paper with the right angle allowed accurate measurement of the stain location using a laser distance finder (Figure 5). The y and z location of the bottom-left corner of the paper on the wall (y = 25 cm, z = 65 cm) was added to the measured location to give the actual location of each stain on the wall. Two analysts performed the measurements while a third recorded the locations.

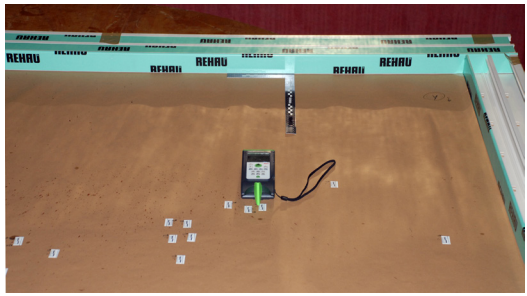

Figure 5

A right-angle border was constructed and a laser distance finder was used to determine stain location.

One analyst performed the analyses on all 32 impact patterns using a special version of the HemoSpat bloodstain pattern analysis software (FORident Software, Inc., Ottawa, Canada). The normal version of HemoSpat only performs calculations for a full two-sided pattern. The special version used the scripting language Lua (freeware available at www.lua.org) to allow scripting of multiple area-of-origin calculations. This allowed us to do a normal, full analysis on each of the patterns and then let the scripts calculate the areas of origin using only positive gammas and only negative gammas. These results were then presented to the analyst in a spreadsheet within HemoSpat (Figure 6) and subsequently exported to OpenOffice (freeware available at OpenOffice.org) for further analysis. Additionally, this special version of HemoSpat displays the puck location in the two-dimensional views of the impact patterns (Figures 7–9).

HemoSpat Experiment Results

Project	Pattern	Result Name	Origin	Deviation	Known Origin	Difference
GS Pattern A	Pattern A	built-in	29.3, 100.2, 88.6	3.4, 2.6, 12.9	30.0, 103.8, 83.0	-0.7, -3.6, 5.6
GS Pattern A	Pattern A	neg gamma side	26.0, 99.1, 90.2	10.7, 7.1, 6.6	30.0, 103.8, 83.0	-4.0, -4.7, 7.2
GS Pattern A	Pattern A	pos gamma side	28.5, 99.8, 94.2	14.5, 15.4, 15.5	30.0, 103.8, 83.0	-1.5, -4.0, 11.2

Figure 6

The experiment version of HemoSpat displays additional results in a spreadsheet.

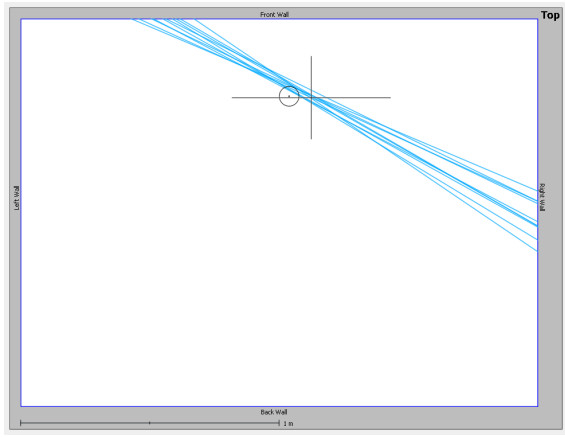

Figure 7

The negative gamma side of pattern "U".
The experiment version of HemoSpat displays the puck location.

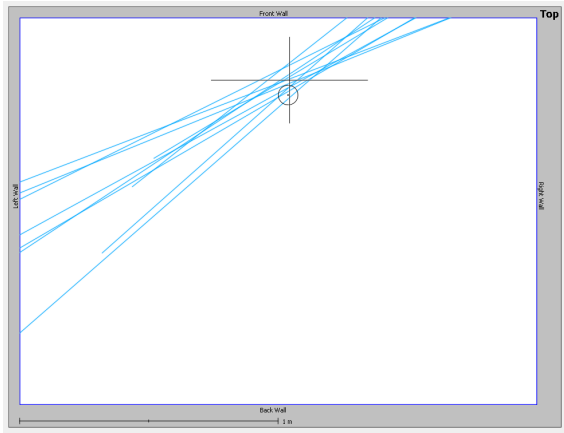

Figure 8

The positive gamma side of pattern "U".
The experiment version of HemoSpat displays the puck location.

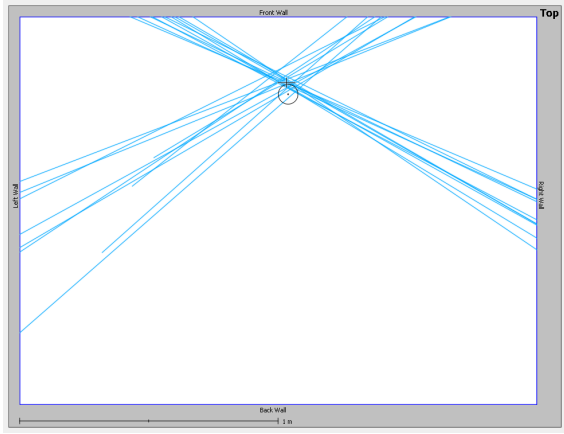

Figure 9

The full two-sided pattern "U".
The experiment version of HemoSpat displays the puck location.

Results and Discussion

Appendix 1 shows each of the 32 patterns – "Pattern A" through "Pattern AF" – and the position and standard deviations for the areas of origin calculated for both the negative gamma side and the positive gamma side. These large standard deviations merit some reflection. The deviations in the z, which range from 3.3 cm to 15.5 cm, are in line with what we see using a complete two-sided analysis, listed in Appendix 2, which ranges from 4.3 cm to 12.9 cm. The deviation in the x and y, however, are larger by an order of magnitude. In the full pattern, the deviations in the x range from 1.6 cm to 3.9 cm, and the deviations in the y range from 1.3 cm to 5.6 cm. In the one-sided patterns, however, the x deviations range from 5.1 cm to 20.5 cm, and the deviations in the y range from 4.8 cm to 45.1 cm.

These large standard deviations may be explained by examining the results of one of the patterns. The trajectories from the negative gamma side and positive gamma side of pattern "U" are shown graphically in Figure 7 and Figure 8, respectively. Although in theory all trajectories should converge to a single point, what we see in practice is that they converge on an area [4] and may have some trajectories almost parallel to each other. It is for this reason that stains are typically chosen from both sides of the pattern – their trajectories cannot be parallel and are more likely to cross closer to the area of origin. Figure 9 shows the top-down trajectories for the full pattern "U".

With any full two-sided analysis, the number of stains selected for analysis may have a dramatic effect on the results. A small number of stains with intersecting trajectories will give a result, but statistically, a larger number – 10 or 15 stains – will give a more accurate result. The same is true for one-sided patterns. The large variations in the x and y standard deviations in Appendix 1 indicate that these one-sided patterns are even more sensitive to the number of stains used for the analysis. Determining how a change in the number of stains affects the results for one-sided patterns is outside the scope of this study and merits its own examination.

As outlined in Maloney et al. [5], when assessing the accuracy of an area-of-origin calculation, there is a range of distances considered acceptable. These range from the size of a tennis ball (approximately 6.5 cm) to 30.5 cm. Table 1 shows the results of the analysis of the full two-sided pattern, just the negative gamma side, just the positive gamma side, and all one-sided patterns together. The known origin of the impact is

x = 30.0 cm, y = 103.8 cm, and z = 83.0 cm. The mean distance from the known origin across all 64 one-sided patterns was x = 24.4 cm, y = 101.6 cm, and z = 89.5 cm. This differs from the known position by 5.6 cm on the x-axis, 2.2 cm on the y-axis, and 6.5 cm on the z-axis. These differences fall well within the range of acceptable limits laid out in the current literature.

	Mean			Standard Deviation			
	x	y	z	x	y	z	(N)
Full Pattern	25.3	101.5	87.9	1.34	2.19	2.92	32
Negative Gamma	24.5	99.8	89.5	3.57	5.40	5.92	32
Positive Gamma	24.3	103.5	89.6	3.43	5.38	5.26	32
All One Sided	24.4	101.6	89.5	3.48	5.65	5.56	64

Table 1

The mean and standard deviation calculated for the full patterns, negative and positive gamma sides, and all one-sided patterns together.

Conclusion

Bloodstain analysts must work with the data they are presented with at the crime scene, regardless of quantity or quality. Sometimes this means eliminating partial impact patterns because too few stains may be found for a regular analysis. This study demonstrates that at least some incomplete impact patterns – "one-sided" patterns – need not be eliminated from the analysis of the scene because they can still provide an acceptable calculation of the area of origin.

In this study, we used a minimum of 10 stains for each one-sided pattern and the results were within the range of acceptable limits. Examining how the number of stains chosen might affect these results would be a logical next step in this line of research.

Acknowledgments

The authors would like to acknowledge L'Institut de Recherche Criminelle de la Gendarmerie Nationale and FORident Software for providing the lab space, materials, and funding for this study. We would also like to thank Terri-Lynne Scott, Research Manager at the Correctional Service of Canada, for her input.

For further information, please contact:

Andy Maloney
FORident Software
207 Bank Street, Suite 132
Ottawa, ON
Canada K2P 2N2
andy@forident.com

References

1. James, S. H.; Kish, P. E.; Sutton, T. P. *Principles of Bloodstain Pattern Analysis: Theory and Practice*, 3rd ed.; CRC Press: Boca Raton, FL, 2005; p 224.
2. Carter, A. L. The Directional Analysis of Bloodstain Patterns Theory and Experimental Validation. *Can. Soc. For. Sci. J.* **2001**, *34* (4), 185.
3. Carter, A. L. The Physics of Bloodstain Pattern Analysis: Lecture Notes; Canadian Police College, Ottawa, Canada, 2005; pp 18, 33.
4. Bevel, T.; Gardner, R. M. *Bloodstain Pattern Analysis: With an Introduction to Crime Scene Reconstruction*, 3rd ed.; CRC Press: Boca Raton, FL, 2008; p 181.
5. Maloney, K.; Killeen, J.; Maloney, A. The Use of HemoSpat to Include Bloodstains Located on Nonorthogonal Surfaces in Area-of-Origin Calculations. *J. For. Ident.* **2009**, *59* (5), 518.

Appendix 1

Calculated positions and standard deviations for both the negative and positive gamma sides of each pattern. The known origin is x = 30.0 cm, y = 103.8 cm, and z = 83.0 cm.

Pattern	Negative Gamma						Positive Gamma					
	x	y	z	sx	sy	sz	x	y	z	sx	sy	sz
Pattern A	26.0	99.1	90.2	10.7	7.1	6.6	28.5	99.8	94.2	14.5	15.4	15.5
Pattern B	20.5	99.4	95.8	8.2	6.6	6.3	20.6	108.2	102.4	13.1	18.5	8.2
Pattern C	27.2	104.5	85.2	11.5	11.4	5.0	21.6	102.5	97.8	6.6	6.3	5.0
Pattern D	20.8	96.7	95.5	5.1	6.7	9.0	25.9	98.3	83.9	10.5	5.1	4.3
Pattern E	23.7	96.4	90.7	14.6	18.7	6.9	23.9	105.4	90.0	14.5	29.8	4.8
Pattern F	23.0	95.9	90.5	11.0	12.1	7.3	25.6	98.7	83.6	9.6	10.8	5.6
Pattern G	28.5	102.9	104.7	15.9	21.4	10.4	33.7	98.6	78.9	20.5	19.1	3.9
Pattern H	27.6	99.9	83.0	12.7	16.2	9.5	22.0	100.8	91.0	8.9	9.7	6.9
Pattern I	25.3	101.1	86.8	10.6	16.2	6.8	28.1	99.7	82.8	11.2	9.1	7.8
Pattern J	27.5	105.5	91.9	18.8	23.6	7.6	29.6	96.7	88.4	11.7	12.6	12.0
Pattern K	22.2	101.6	88.3	15.0	32.0	7.6	23.3	109.0	90.7	15.7	23.9	9.0
Pattern L	26.4	107.0	82.2	11.0	18.4	9.1	24.9	106.0	93.9	15.0	17.9	4.9
Pattern M	30.2	106.4	79.3	17.6	23.9	7.3	21.0	112.2	93.2	13.9	24.7	8.3
Pattern N	27.0	101.0	82.3	9.8	15.4	6.6	25.8	99.9	84.7	13.0	16.8	8.6
Pattern O	26.7	104.3	85.9	14.1	24.2	7.9	22.1	108.2	89.6	10.7	15.1	6.8
Pattern P	29.6	108.6	84.9	15.5	19.7	8.1	22.1	107.8	93.3	11.5	18.2	5.9
Pattern Q	23.0	97.4	90.5	13.9	24.3	5.2	25.3	101.1	88.1	13.3	21.7	3.3
Pattern R	20.9	96.2	95.0	10.5	19.1	6.9	24.7	101.3	91.0	8.3	6.7	6.8
Pattern S	22.3	100.7	87.8	15.4	13.4	7.0	22.9	106.3	90.3	12.0	18.1	5.1
Pattern T	17.9	89.2	96.2	18.0	30.7	4.7	23.5	102.8	89.2	15.9	26.3	9.6
Pattern U	30.6	112.4	86.8	16.0	30.6	6.9	27.2	98.8	82.3	16.9	30.0	8.3
Pattern V	30.4	104.0	80.3	14.3	4.8	10.7	21.0	105.7	95.9	11.1	11.4	6.7
Pattern W	24.8	100.2	80.9	9.3	9.2	14.5	24.7	102.5	89.2	14.2	25.0	4.1
Pattern X	22.5	94.4	88.2	18.9	45.1	4.7	21.2	104.2	89.1	12.5	24.2	5.0
Pattern Y	24.9	101.4	88.8	15.2	17.2	4.8	25.6	108.5	90.0	14.5	19.8	5.8
Pattern Z	20.1	94.2	91.4	15.2	19.6	5.8	24.2	109.8	87.2	15.0	24.7	3.5
Pattern AA	21.7	91.9	95.4	10.5	15.8	9.2	19.0	109.3	94.5	14.0	20.7	5.9
Pattern AB	21.1	98.5	90.6	8.3	9.0	5.7	31.4	88.2	78.9	16.4	30.7	5.4
Pattern AC	20.0	96.9	90.5	13.6	22.2	8.4	21.3	107.9	91.1	12.8	23.6	3.7
Pattern AD	18.9	87.4	102.5	16.8	26.9	6.9	20.4	112.1	94.3	12.4	24.3	8.4
Pattern AE	25.1	98.2	90.1	19.4	27.7	6.4	26.1	95.0	84.7	13.8	28.8	7.9
Pattern AF	27.6	101.1	90.4	9.8	14.8	4.8	19.7	105.8	93.0	9.9	18.6	4.1

Appendix 2

Calculated position and standard deviation for each full pattern. The known origin is x = 30.0 cm, y = 103.8 cm, and z = 83.0 cm.

Pattern	Full Pattern					
	x	y	z	sx	sy	sz
Pattern A	29.3	100.2	88.6	3.4	2.6	12.9
Pattern B	23.4	103.2	94.0	2.8	3.1	7.5
Pattern C	23.2	101.7	92.3	2.3	1.7	5.2
Pattern D	22.9	99.2	89.3	1.7	1.3	7.6
Pattern E	25.3	101.5	87.9	2.6	4.5	6.0
Pattern F	25.5	99.4	84.9	2.3	2.3	6.6
Pattern G	28.7	102.5	94.4	2.6	2.9	12.7
Pattern H	25.0	97.2	85.7	3.9	4.4	7.6
Pattern I	26.5	101.0	85.4	3.1	2.2	7.3
Pattern J	25.5	101.5	94.4	2.8	3.2	9.7
Pattern K	24.3	107.1	87.0	2.8	5.6	8.7
Pattern L	24.8	105.3	89.6	1.6	2.1	8.0
Pattern M	26.2	101.2	85.2	3.1	5.3	7.1
Pattern N	25.1	98.8	85.8	2.6	3.3	7.2
Pattern O	26.0	102.9	86.2	2.8	3.7	6.2
Pattern P	24.9	102.1	91.1	2.7	3.7	6.8
Pattern Q	24.7	101.4	88.9	1.7	2.8	4.3
Pattern R	24.8	101.5	89.3	2.9	2.9	7.5
Pattern S	24.7	102.3	86.2	2.3	2.7	7.0
Pattern T	25.9	101.9	86.8	3.6	5.6	7.4
Pattern U	25.2	102.6	88.7	1.9	3.6	7.7
Pattern V	25.0	102.6	88.9	2.8	1.4	8.5
Pattern W	25.2	100.7	84.3	1.9	2.5	11.3
Pattern X	24.3	98.2	84.8	2.6	5.3	5.2
Pattern Y	27.2	105.3	86.5	2.7	3.4	5.7
Pattern Z	26.4	104.0	82.7	2.0	3.1	5.8
Pattern AA	25.6	99.2	86.0	3.1	4.9	8.9
Pattern AB	24.3	101.6	87.5	2.1	3.0	5.5
Pattern AC	24.6	103.7	85.2	3.4	5.5	7.3
Pattern AD	26.2	101.2	87.7	1.8	3.2	7.7
Pattern AE	24.8	99.4	88.6	2.4	4.2	7.2
Pattern AF	24.8	98.5	88.8	2.4	3.9	6.4